Optimization of Flame Retardant System for Waste Tetra Pak/Bamboo Fiber Composites with Inorganic Flame Retardants

Huijie Zhang,^a Hui Guo,^a Yufei Cai,^a Hui Li,^{b,c,*} Dezhi Zhou,^d Binqing Sun,^a and Lili Yu ^{a,*}

Tetra Pak (TP)/bamboo fiber (BF) composites were prepared using waste TP and bamboo fiber as the main raw materials. Twelve inorganic flame retardant systems were used to modify the flame retardancy of TP/BF composites. Specimens were evaluated with the limiting oxygen index test, water absorption test, dry shrinkage and wet expansion test, mechanical property test, and Fourier transform infrared spectroscopy (FTIR). The results showed that the composite flame retardant systems outperformed the single flame retardant system, with the limiting oxygen index reaching up to 37.6%. Retardant addition lowered the modulus of elasticity (MOE), modulus or rupture (MOR), and internal bond (IB) and impaired dimensional stability, the extent varying with type and dosage. Among them, the TP/BF composites modified by systems Z3, Z8, Z9, and Z12 satisfied GB/T 11718-2021 requirements for ordinary, furniture, and building medium-density fiberboards. FTIR showed the presence of chemical bonds of various functional groups that would be consistent with the development of adhesion within the composite.

DOI: 10.15376/biores.20.4.10228-10248

Keywords: Waste Tetra Pak fiber; Bamboo fiber; Flame retardant; Mechanical properties; Dimensional durability

Contact information: a: College of Light Industry Science and Engineering, Tianjin University of Science & Technology, Tianjin 300457, China; b: Hubei Academy of Forestry, Wuhan430075, China; c: Hubei Mufushan Mountain Bamboo Forest Ecosystem Research Station, Xianning437100, Hubei, China; d: Wuxi Qiancheng Packaging Engineering Co., Ltd., Jiangsu 214112, China;

* Corresponding authors: 827231442@qq.com; 24823925@mail.tust.edu.cn

INTRODUCTION

Tetra Pak has played a significant role in the packaging industry, helping to ensure product freshness without preservatives by blocking light, air, and contaminants, significantly extending shelf life. Additionally, the multi-layered material structure could provide superior protection while maintaining nutritional value and flavor integrity (Baskoro *et al.* 2017; Muñoz-Vélez *et al.* 2018). Tetra Pak cartons are widely used in the global beverage and dairy industries, and they account for approximately 70% of the food packaging market share. Typically, a standard Tetra Pak carton features a multi-layer composite structure, mainly consisting of food-grade polyethylene (PE) layers (for waterproofing and sealing), a paperboard layer (for structural support), and a thin aluminum layer (for enhancing barrier performance against oxygen, light, and moisture). This "paper-aluminum-plastic" laminated structure is the core reason for its excellent

protective properties, but it also brings challenges related to subsequent waste disposal. As the result, the disposal of waste Tetra Paks has become a research hotspot (Martínez Barrera and Escobar Campos 2024). At present, most of the cartons are disposed of by landfilling or incineration as garbage. Landfilling involves collecting waste Tetra Paks and taking them to waste yards or conducting deep landfills, allowing them to degrade under natural conditions, which is a rather passive approach. Large-scale recycling and degradation of waste Tetra Paks require large-area waste yards, resulting in high recycling costs. Moreover, the polyethylene in Tetra Paks has stable properties, and the natural degradation time in soil is extremely long. This method is currently common in small and medium-sized cities and along railway lines, but it is gradually being replaced by other recycling and disposal methods because it is not conducive to the long-term development of the ecology (Khalil et al. 2016; Ye et al. 2022). Incineration is a fast and effective method for handling waste Tetra Paks, which has a simple process and does not require pre-treatment, and is currently often used for thermal power generation. Although this treatment method can obtain high-value energy, the incineration process easily produces a large amount of toxic gases, causing pollution to the environment (Amorim et al. 2024). Therefore, converting waste Tetra Paks into new composite materials with certain practical value that are low-carbon and environmentally friendly has important practical significance for both the economy and the environment.

It is reported that a 250 mL "brick-shaped" Tetra Pak weighs approximately 10 grams, and recycling 1 ton of such composite packaging materials can save 11 trees with a 10-year growth period, 0.3 tons of petroleum, or 7.5 tons of bauxite (Ye et al. 2022). However, because of its multi-layered construction, the paper-aluminum-plastic laminate in Tetra Paks is formed by high-frequency and hot-press lamination. As a result, the aluminum layer and LDPE plastic are tightly bonded together, making it difficult to effectively separate them into different components, which impedes the reuse of materials that compose the waste Tetra Paks (Ebadi et al. 2016; Aranda-García et al. 2020). At present, the recycling and utilization of waste Tetra Pak can be generally divided into two categories: separate utilization and integral utilization. The separation and utilization technology involves peeling off the paper fibers, plastics, and aluminum foils in Tetra Paks for respective reuse, mainly including hydraulic recycled pulp technology and plastic-aluminum separation technology. Hydraulic recycled pulp technology separates paper fibers from aluminum-plastic materials through hydraulic stirring. The next step is to obtain high-quality long-fiber pulp through processes such as rinsing, precipitation, centrifugation, and filtration. The cardboard layer in waste Tetra Paks, after absorbing water, leads to a decrease in the binding force of fibers. Through stirring, the cardboard layer is separated from other components. Meanwhile, the wastewater generated during the production process can be reused after primary sedimentation treatment. The recovered long-fiber pulp can be reused in the production of various paper products, and the obtained aluminum components can be applied in the field of adsorption (Riedewald et al. 2022; Amorim et al. 2024). Zúñiga-Muro et al. (2021) recovered coke and aluminum from Tetra Pak waste using hydraulic recycled pulp technology and thermal degradation process. The study found that the recovered aluminum with different physical and chemical properties and oxide/ hydroxide compositions, as well as the coke with low porosity and surface oxygen-containing functional groups, can be used as adsorbents to remove mercury from aqueous solutions. Plastic-aluminum separation is usually a by-product after paper-plastic separation. The aluminum-plastic screen residues after removing pulp are processed by chemical and physical methods to obtain raw materials for producing plastics and aluminum products. Frank *et al.* (2022) used a molten metal pyrolysis reactor to recover aluminum from waste Tetra Pak packaging, and the experimental results showed that this technology can effectively recover clean aluminum. Ding *et al.* (2018) used waste Tetra Paks as raw materials, conducted acid pretreatment and slow pyrolysis in an oxygen-limited environment at 600 °C to prepare low-cost aluminum-rich biochar, which has good adsorption performance for As(III) and As(V). However, this method also has problems such as expensive equipment, complex processes, difficulty in completely peeling off the packaging containers, and secondary pollution in many processes (Li *et al.* 2024a; Liu *et al.* 2024).

The integral utilization technology involves using discarded Tetra Pak as raw materials without component separation. Through processing techniques such as crushing, extrusion, molding, and injection molding, they are made into composite panels. The high proportion of cellulose fibers in the panels helps maintain the shape of the composite material, and the multi-layer structure separated by aluminum sheets can help improve the barrier performance of the cardboard and reduce the heat transfer of the material (Bekhta *et al.* 2016; Aranda-García *et al.* 2020). Ebadi *et al.* (2016) found that the composites containing 30% of Tetra Pak and 3% maleic anhydride-grafted polyethylene (MAPE) achieved the highest strength and tensile modulus for the wood–plastic composites. Kolyada *et al.* (2021) pointed out that the introduction of PVA polyethylene glycol suspension could remarkably enhance the density and mechanical properties of the composites prepared by waste Tetra Pak packaging/wood plastic. Bal (2022) used recycled polyethylene, waste Tetra Pak, and pine wood flour mixed as fillers to produce composite boards with performance meeting standard requirements, indicating that waste Tetra Pak can replace wood flour as a filler in the production of wood-plastic composites.

Bamboo not only has advantages such as a short growth cycle, high strength, good toughness, and strong plasticity, but also boasts abundant resources and favorable ecological benefits (Dou et al. 2011; Wang 2020). As an ideal substitute for wood, it can effectively mitigate the negative impacts of wood resource shortages. The preparation of bamboo-based composite materials by combining waste Tetra Pak can replace traditional wood-based panels for application, which not only saves wood resources, but more importantly, provides a new approach for the recycling and reuse of waste Tetra Pak boasting favorable economic and ecological benefits. The authors' previous research work had investigated the influences of various factors in the preparation of TP/BF composite by single-factor experiments and orthogonal experiments, and the optimal preparation process parameters were determined as follows: hot-pressing temperature of 180 °C, hot-pressing time of 16 minutes, hot-pressing pressure of 1.0MPa, glue application amount of 12%, and Tetra Pak/bamboo ratio of 9:1. Under these conditions, the prepared composite materials met the performance requirements specified in GB/T 11718 (2021) for ordinary, furniture-type and construction-type medium-density fiberboards when used in dry, humid, high-humidity and outdoor conditions (Jiang et al. 2025).

Tetra Pak contains a thin aluminum layer. Aluminum has a melting point of 660 °C, and at room temperature, a dense aluminum oxide (Al₂O₃) film with a melting point of 2072 °C is rapidly formed on its surface, which can effectively isolate oxygen. When the temperature rises to 660 °C, aluminum melts; if heating continues to the range 600 to 800 °C, aluminum first softens, causing the surface oxide film to crack. Under

such circumstances, aluminum will burn in an open space (with sufficient oxygen) or in the presence of strong oxidants (Santhanam *et al* 2010). Especially when aluminum is crushed into powder, its high specific surface area reduces the barrier ability of aluminum oxide, making it easier for aluminum to be integrally heated to the reaction temperature. The product of aluminum foil combustion is aluminum oxide, which does not directly form a carbon layer. If a carbon layer exists, it only results from the pyrolysis and carbonization of paper fibers (from Tetra Pak) and bamboo fibers (*e.g.*, bamboo fibers in TP/BF composites) under oxygen-deficient and medium-low temperature conditions, having no direct connection with aluminum combustion (Dreizin *et al* 1999). Moreover, a continuous carbon layer is difficult to form in actual open combustion environments. Only when the temperature exceeds 800 °C and oxygen is sufficient will aluminum burn violently.

However, since bamboo fiber as well as waste Tetra Pak have strong combustion characteristics, the TP/BF composite should be modified with reasonable flame retardants. Among of them, inorganic flame retardants due to their advantages such as non-toxicity, non-corrosiveness, low price, and smoke suppression have been shown to effectively improve the flame retardancy of the panels and promote their safe and wide application (Guo et al. 2019; Nie et al. 2022). Guo et al. (2019) showed that boric acid can promote the carbonization of bamboo-based epoxy resin composites, thereby significantly improving the flame-retardant performance of the composites. Fang et al. (2020) found that when adding a compound flame retardant of melamine pyrophosphate and aluminum hypophosphite to bamboo fiber/polypropylene composites, the flame-retardant ability increased with the increase in the content of the flame retardant, but the tensile properties of the composites gradually decreased, and the flexural strength and modulus first increased and then dropped sharply. Wang et al. (2020) used silane-coated ammonium polyphosphate as a flame retardant to modify the flame retardancy of bamboo powder/polypropylene composites. Their study also found that as the amount of ammonium polyphosphate was increased, the flame-retardant performance of the composites continues to improve, while the flexural and tensile strengths decreased.

The objective of this study was to evaluate the effects of different inorganic flame retardant systems on the dimensional stability, mechanical properties and flame retardancy of Waste Tetra Pak/bamboo fiber composites, and based on the research results, to provide technical guidance for the recycling of waste Tetra Pak materials.

EXPERIMENTAL

Materials

Waste Tetra Pak packaging of milk within the past three months was collected and washed. After drying, it was cut and shredded into fibrous material. Bamboo was harvested from Dechang City, Sichuan Province. It was crushed into powder and then screened using a 40-mesh sieve. Phenolic resin was purchased from Taier Adhesive Co., Ltd. in Guangdong Province, and its solid content was 43.0%. Emulsified wax was purchased from Shenghui Flame-Retardant Materials Co., Ltd in Gu'an with a solid content of 37.2%, a surfactant content of 11.8%, a viscosity of 26 s (measured by a Coating - 4 Cup), and a pH value of 3.2. Boric acid, borax, and trisodium phosphate were supplied by Tianjin Damao Chemical Reagent Factory. Nano-silica dioxide and

aluminum hydroxide were obtained from Shanghai Aladdin Bio-Chem Technology Co., Ltd. Magnesium hydroxide was provided by Shanghai Biode Pharmaceutical Technology Co., Ltd. Polyphosphoric acid was sourced from Shanghai Macklin Biochemical Co., Ltd. Sodium tetrahydrate diborate was acquired from Shanghai Titan Technology Co., Ltd. Anhydrous ethanol was supplied by Jiangsu Aikang Biopharmaceutical R&D Co., Ltd. Potassium bromide was obtained from Shanghai Jizhi Bio-Technology Co., Ltd.

Preparation of Inorganic Flame Retardants

As illustrated in Table 1, five types of flame retardants, namely boric acid/borax (BBX), nano silicon dioxide (n-SiO₂), magnesium hydroxide/aluminum hydroxide (MH/ATH), ammonium polyphosphate (APP), and disodium octaborate tetrahydrate (DB), as well as seven compounded flame retardants based on these, were employed for the preparation of flame retardants. The influence of different flame retardant components on the flame retardant resistant of composite panels was explored to identify the flame retardant formulation with superior flame retardant capability. Given the poor dispersibility of n-SiO₂ in water, trisodium phosphate (TSP) was chosen as the dispersant for n-SiO₂.

In the process of preparing the flame retardants, the mass fraction of each flame retardant solution was set as its maximum solubility in water. Specifically, under certain temperature conditions, after being uniformly stirred by a magnetic stirrer, the flame retardant solution system remained stable without precipitation at this maximum concentration.

Group No.	Flame Retardant Type	Reagent Mass Fraction (wt%)
Z0	No treatment	
Z1	Boric Acid/Borax	20:20
Z2	n-SiO ₂	1
Z3	Magnesium Hydroxide/Aluminum Hydroxide	1:1
Z4	Ammonium Polyphosphate	2
Z5	Disodium Octaborate Tetrahydrate	10
Z6	Boric Acid/Borax/Ammonium Polyphosphate	20:20:2
Z 7	Boric Acid/Borax/Disodium Octaborate Tetrahydrate	20:20:10
Z8	Boric Acid/Borax/Ammonium Polyphosphate/Disodium Octaborate Tetrahydrate	20:20:2:10
Z 9	Boric Acid/Borax/n-SiO ₂	20:20:1
Z10	Boric Acid/Borax/Magnesium Hydroxide/Aluminum Hydroxide	20:20:1:1
Z11	Boric Acid/Borax/n-SiO ₂ /Magnesium Hydroxide/Aluminum Hydroxide	20:20:1:1:1
Z12	Boric Acid/Borax/Ammonium Polyphosphate/DisodiumOctaborate Tetrahydrate/n-SiO ₂ /Magnesium Hydroxide/Aluminum Hydroxide	20:20:2:10:1:1:1

Preparation of Flame-retardant TP/BF Composites

Tetra Pak cartons(TP) used for dairy products were collected over a three-month period. First, they were manually cleaned and then dried in a convection drying oven. Subsequently, a plant crusher was used to grind them into fibrous fragments. Bamboo

filaments(BF) were ground into bamboo powder using a cutting grinder; after removing impurities, the bamboo powder was sieved through a 40-mesh screen, sub-packaged, and then dried to a constant weight in a blast drying oven.

TP fiber and bamboo fiber with the mass ratio of 9:1 were immersed in the solution of different flame retardants as illustrated in Table 1, and the composite without any flame retardants was used as the control group (Z0). The flame retardant-modified fibers were dried in a convection drying oven at a temperature of 103 ± 2 °C until the moisture content reached 5%, which were mixed evenly with 12% of phenolic resin adhesive in a small mixer. After that, these experimental materials were spread in a 250 mm × 250 mm × 4 mm mold. They were hot-pressed at 180 °C, 1.0 MPa, for 16 min to prepare flame-retardant TP/BF composites. The TP/BF composite panels were evaluated for flame retardant properties and mechanical properties, respectively. The process is shown in Fig. 1.

Mechanical Performance

TP/BF composites were tested to determine the modulus of rupture (MOR), modulus of elasticity (MOE), and internal bonding strength (IB) according to GB/T 11718 (2021).

MOR

The specimens with dimensions of 200 mm × 50 mm × 10 mm were placed on the support, and the distance between the two supports was set to 64 mm. Five repeated samples were used in each group. The flexural deformation of the specimens was measured, and the test load corresponding to this flexural deformation was recorded. A load-deflection curve was plotted based on the flexural deformation and the corresponding load values. The MOR of the specimen was calculated using Eq. 1,

$$\sigma_b = \frac{3 \times F_{max} \times l_1}{2 \times b \times t^2} \tag{1}$$

where σ_b is the MOR of the specimen (MPa), F_{max} is the maximum load at specimen failure (N), l_1 is the distance between the two supports (mm), b is the width of the specimen (mm), and t is the thickness of the specimen (mm).

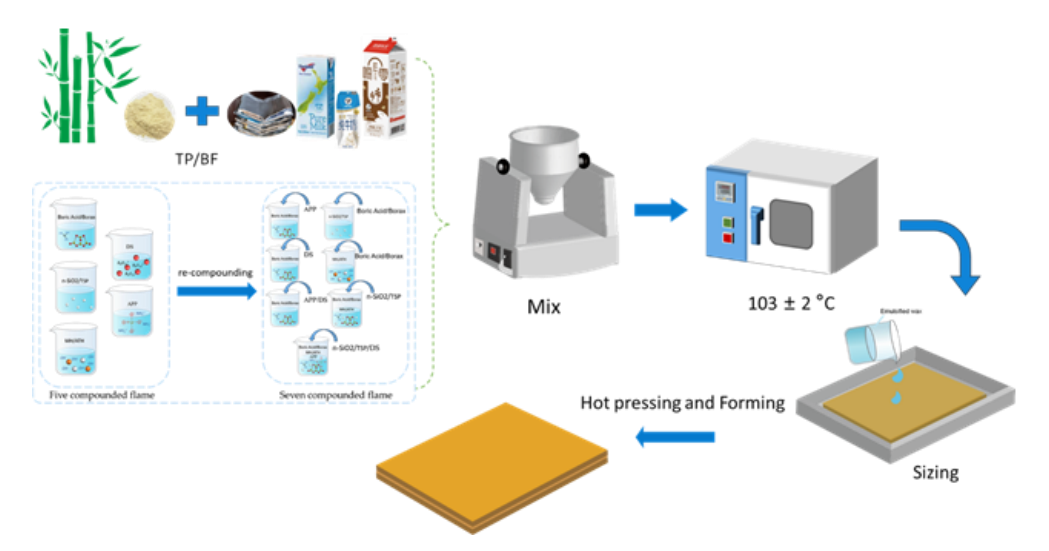


Fig. 1. Flowchart for the preparation of TP/BF composites

MOE

The elastic modulus (MOE) of the specimens was calculated as follows,

$$E_b = \frac{l_2^3}{4 \times b \times t^3} \times \frac{F_2 - F_1}{a_2 - a_1} \tag{2}$$

where E_b is the MOE of the specimen (MPa), l_1 is the distance between the two supports (mm), b is the width of the specimen (mm), t is the thickness of the specimen (mm), F_{2} - F_{1} is the increase of the load in the linear section of the load-deflection curve (F_{1} value is about 10% of the maximum load, F_{2} value is about 40% of the maximum load) (N), and a_{2} - a_{1} is the increase of the deformation in the middle of the specimen, that is, the deformation of the specimen in the F_{2} - F_{1} interval (mm). The arithmetic mean of the elastic moduli of all specimens (two groups of longitudinal and transverse specimens) from the same composite is taken as the elastic modulus of the composite.

Internal bonding strength

The specimens with dimensions of 50 mm \times 50 mm \times 10 mm were glued to the chuck, and the hot melt adhesive was evenly coated on the surface of the chuck, so that they could be closely integrated. The glued composite was placed in the clamping device of the testing machine. An appropriate loading speed was selected for constant-speed loading. The specimen was broken within 90 s, and the maximum load value was recorded. The internal bonding strength (σ_{\perp}) of the specimen was calculated as follows,

$$\sigma_{\perp} = \frac{F_{max}}{l \times b} \tag{3}$$

where F_{max} is the maximum load when the specimen is broken (N), l is the length of the specimen (mm), and b is the width of the specimen (mm).

Dimensional Stability

Extents of water absorption and thickness swelling

According to GB/T 11718 (2021), the specimens with the dimensions of 50 mm \times 50 mm \times 10 mm were conditioned to a constant weight at 23 \pm 2 °C and a relative humidity (RH) of 50 \pm 5% to reach the equilibrium moisture content of 7 to 8%. Deionized water was poured into a constant-temperature water bath to maintain the water temperature at 20 \pm 1 °C. The specimens were immersed in the water with the upper part of the specimens 30 mm below the water surface and the surface of the specimens perpendicular to the water surface. The extent of thickness swelling (TS) was calculated by Eq. 4,

$$TS = \frac{t_2 - t_1}{t_1} \times 100\% \tag{4}$$

where t_1 and t_2 are the thickness of specimens before immersing into water and after 7 days of immersion into water, respectively.

The 24h water absorption extent (WA) was calculated using Eq. 5,

$$WA = \frac{m_2 - m_1}{m_1} \times 100\% \tag{5}$$

where m_1 and m_2 are the mass of the specimen before and after water immersion, respectively.

Wetting swelling and drying shrinkage

According to GB/T 11718 (2021), samples were conditioned at 20 ± 2 °C and RH of $30 \pm 5\%$ to reach constant weight, then conditioned at 20 ± 2 °C and RH of $65 \pm 5\%$ to reach constant weight, and finally conditioned at 20 ± 2 °C and RH of $85 \pm 5\%$ to reach constant weight for a third time. The swelling extents in length and thickness were calculated according to the following equations,

$$\Delta l_{65,85} = \frac{l_{85} - l_{65}}{l_{65}} \times 1000 \tag{6}$$

$$\Delta t_{65,85} = \frac{t_{85} - t_{65}}{t_{65}} \times 100 \tag{7}$$

where $\Delta l_{65,85}$ is the relative change in length when the relative humidity is within the range of 65% to 85% (mm/m), l_{65} is the length between the measurement points at 20 ± 2 °C and relative humidity of $65 \pm 5\%$, l_{85} is the length between the measurement points at 20 ± 2 °C and RH of $85 \pm 5\%$. $\Delta t_{65,85}$ is the relative change in thickness when the RH is within the range of 65% to 85% (mm/m), t_{65} is the thickness between the measurement points at 20 ± 2 °C and RH of $65 \pm 5\%$, and t_{85} is the thickness between the measurement points at 20 ± 2 °C and RH of $85 \pm 5\%$.

To test shrinkage in drying, samples were firstly conditioned at 20 ± 2 °C and RH of $85 \pm 5\%$ to reach constant weight, then conditioned at 20 ± 2 °C and RH of $65 \pm 5\%$ to reach constant weight, and finally conditioned at 20 ± 2 °C and RH of $30 \pm 5\%$ to reach constant weight. The shrinkage extents in length and thickness were calculated as follows,

$$\Delta l_{65,30} = \frac{l_{30} - l_{65}}{l_{65}} \times 1000 \tag{8}$$

$$\Delta t_{65,30} = \frac{t_{30} - t_{65}}{t_{65}} \times 100 \tag{9}$$

where $\Delta l_{65,30}$ is the relative change in length when the RH is within the range of 65% to 30% (mm/m), and l_{30} is the length between the measurement points at 20 ± 2 °C and RH of (30±5)%. $\Delta t_{65,30}$ is the relative change in thickness when the RH is within the range of 65% to 30% (mm/m), and t_{30} is the thickness between the measurement points at 20 ± 2 °C and RH of (30±5)%.

Limiting Oxygen Index Determination

Limiting oxygen index (LOI) tests were performed according to GB/T 2406.2 (2009) using an KS-653B oxygen index meter (Jinsen Analytical Instrument, Shanghai, China). The samples were dried at 103 ± 2 °C until reaching constant weight. A total of 15 replicates with the dimensions of 100 mm \times 10 mm \times 3 mm were prepared for each group of the samples.

Fourier Transform Infrared Spectroscopy (FT-IR) Analysis

The samples were detected using a Nicolet 6700 Fourier Transform Infrared Spectrometer produced by Thermo Electron Corporation, Madison, WI, USA. Approximately 2 mg of the samples with different treatments with a particle size of 100 mesh was weighed and mixed with about 160 mg of KBr powder and then ground into fine powder in an agate mortar many times, dried, and pressed into tablets. Finally, the tableted samples were put into the sample chamber, and the iD1 mode was used to scan 16 times with a resolution of 4 cm⁻¹, and the test scan range was 4000 to 500 cm⁻¹.

RESULTS AND DISCUSSION

Flame Retardancy Analysis

The limiting oxygen index (LOI) values of TP/BF composites with different flame retardants and without flame retardant are shown in Fig. 2. Although the phenolic resin adhesive used in the preparation of TP/BF composites exhibited certain flameretardant effects (Li et al. 2023a), the LOI value of the Z0 group composite was only 27.3%, which was still classified as a B2-grade combustible material according to GB 8624 (2012). The Z1 and Z3 groups treated with boric acid/borax and disodium octaborate tetrahydrate, respectively, achieved an LOI values of 32.3% and 34.5%, reaching a B1-grade difficult-to-burn material (above 32%), which was attributed to the condensed phase and gas phase flame retardant mechanisms of boron-based flame retardant systems (Kumar et al. 2022; Ünal et al. 2023). The Z2 group with nano-silica showed an LOI value similar to that of the Z0 group, indicating that the nano-silica did not enhance the flame retardancy of the composite. This may be due to the low content of nano-silica, which was insufficient to achieve effective flame retardancy. The Z3 group treated with magnesium hydroxide/ aluminum hydroxide (MH/ATH) had an LOI value of only 31.9%, but the smoke emission during combustion was significantly reduced. This was mainly attributed to the fact that ATH and MH could decompose endothermically during combustion, and their residues cover the surface of the composite, further inhibiting combustion (Kongkraireug et al. 2018; Lan et al. 2018).

The Z4 group treated with ammonium polyphosphate (APP) achieved an LOI of 36.2%, demonstrating a significant improvement in flame retardancy, which was because APP was an intumescent flame retardant. On the one hand, when heated, APP promoted the dehydration and carbonization of polymer chains, forming a dense char layer that slowed heat transfer. The char effectively isolated the condensed phase from the gas phase, thereby preventing the entry of external oxygen and the release of flammable volatile gases. On the other hand, its thermal decomposition produced non-combustible gases such as NH₃, NO, and water vapor, which not only diluted the concentration of flammable gases in the air but also caused the char layer to expand, which reduced heat and mass transfer rates (Li and Lv 2022; Li *et al.* 2024b). However, during combustion tests, this group exhibited significantly higher smoke emission compared to other groups, which was likely because APP decomposes into polyphosphoric acid and ammonia, which then react with water vapor and particulates in the air to form smoke (Shi 2017).

From the LOI results of the Z6, Z7, Z8, Z9, Z10, Z11, and Z12 groups, it could be seen that the LOI values of these composites ranged between 34.5% and 37.6%. Compared to the single flame-retardant systems (Z1, Z2, Z3) except for Z4, the flame retardancy of these composites was significantly improved, which indicated that different inorganic flame-retardant systems could exhibit a synergistic effect during combustion of the composite (Liu 2018; Meng 2020; Zhao 2024), particularly the combination of nanosilica with other flame retardants, which significantly enhanced the overall flame retardancy of the composite. However, the combination of APP with other inorganic flame retardants did not notably improve the flame retardancy and even slightly reduced the LOI value, though it significantly reduced smoke emission.

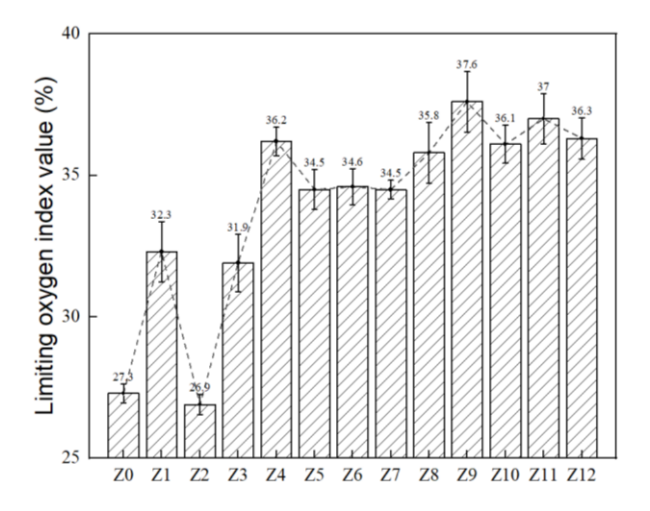


Fig. 2. Effect of different flame retardants on limiting oxygen index value of TP/BF composites Water absorbency analysis

Figure 3 shows the effects of different flame-retardant systems on the water absorbency and of TP/BF composites. Compared with the untreated group, the 24 h water absorption thickness swelling of all the treated samples decreased in the wide range of 11.3% to 137.8%, and the huge difference was attributed to the nature of different flame retardant systems, the addition amount of flame retardant, and the compatibility of the flame retardant with the composite matrix. The flame retardant in the TP/BF composite

would enter the pore structure of the composites, reducing the number and size of the pores in the composites, which would diminish the infiltration and diffusion of water in the composites. Therefore, the overall performance showed that the water absorption by the composite decreased after flame retardant treatment. In the Z1 group, the 24-h water absorption thickness swelling of the composites increased, which was mainly caused by the addition of boric acid/borax hindered the adhesion between the fibers and the glue. As the duration of water immersion increased, the boric acid/borax attached to the fiber surface was easily dissolved in water, and the adhesive gradually lost its adhesion ability due to hydrolysis. As a result, the fibers rebounded in their dimensions due to stress release after being affected by moisture (Li and Xu 2008; Lu and Lu 2023). In the Z2 group, the aqueous solution of trisodium phosphate was strongly alkaline due to the strong hydrolysis of phosphate ions. The alkali treatment would dissolve and remove some non-fiber substances such as pectin and wax on the surface of bamboo components, resulting in voids in the composite structure, which was manifested as the expansion of the composite structure after water absorption (Chen 2011; Zhou 2018). In the Z3 and Z4 groups, the thickness expansion of the composites was mainly due to the poor interfacial compatibility between the flame retardant components and the matrix, resulting in a decrease in the bonding ability of the composites. At the same time, the resilience of the fibers after water absorption exceeded the remaining adhesion of the adhesive after hydrolysis. In the Z5 group, the flame retardant disodium octaborate tetrahydrate attached to the fibers was easily dissolved in water, and the aqueous solution was alkaline, resulting in the formation of pores in the composites and causing thickness expansion. In the Z6 to Z12 groups, the TP/BF composites treated with multi-component flame retardant compounding, and the thickness swelling was also changed due to the different types and contents of the flame retardants.

Compared with the untreated group, the water absorption by the treated samples decreased significantly. This might be attributed to the fact that after the flame retardant was added, it would enter the pore structure of the TP/BF composite material, reducing the number and size of pores in the composite material. As a result, the penetration and diffusion of the total content of water inside the composite after long-term immersion was inhibited effectively. Lower water absorption values were observed in the groups of Z2, Z3, Z4 and Z9, and the higher water absorption was observed in the groups of Z7, Z8, and Z10. This demonstrated that different inorganic flame retardants and the corresponding combinations would exhibit different effects on the water absorption performance on the composites.

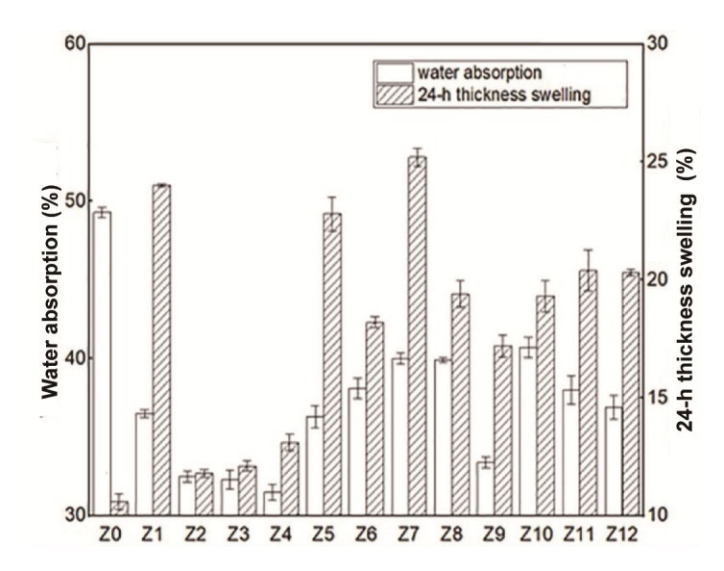


Fig. 3. Effect of different flame retardants on water absorbency of TP/BF composites wetting swelling and drying shrinkage properties analysis

Figure 4 shows the effects of different flame-retardant systems on the shrinkage and swelling property of TP/BF composites under the conditions of changing ambient RH. When the RH increased from 65% to 85%, or from 65% to 30%, compared with the untreated samples (Z0), the length and thickness of the treated samples changed significantly, which was mainly because all of the inorganic flame retardants selected in this study had some certain hygroscopicity resulting in the phenomena of hygroscopic expansion and drying shrinkage of the composites. During the moisture absorption or evaporation process, the changes in the length and thickness directions of the samples with different inorganic flame retardant systems showed different degrees of differences, especially for the groups of Z1, Z6, and Z12. The changes in the length direction were much higher than those in other groups, which demonstrated that both the components of the flame retardants and the combination of different flame retardants would affect the shrinkage and swelling performance of TP/BF composites. The change of length was higher than that of thickness in the TP/BF composite with the vast majority of flame retardant modification conditions as the RH in the surrounding environment changed. This was primarily due to factors such as fiber orientation and possible density variations along the thickness direction of the composite. During the forming process, the composite typically exhibited a certain degree of orientation, with more fibers aligned along the length direction. As a result, when the composite absorbed or lost moisture, the fibers expanded or contracted due to hygroscopic or drying effects, leading the overall dimensional change in the length direction. Specimens having more interconnected fibers exhibited more shrinkage or expansion (Way et al. 2020; Liu et al. 2021; Li et al. 2023b). For the TP/BF composite, the density variations along the thickness direction of the composite were inevitable. Typically, higher density was observed at the surface and lower density was observed in the core. As a result, the dimensional change would be subject to more constraints, which limited the range of its dimensional changes. Meanwhile, in the length direction, the density was relatively uniform, therefore exhibiting more consistent moisture effects, making shrinkage and expansion more noticeable.

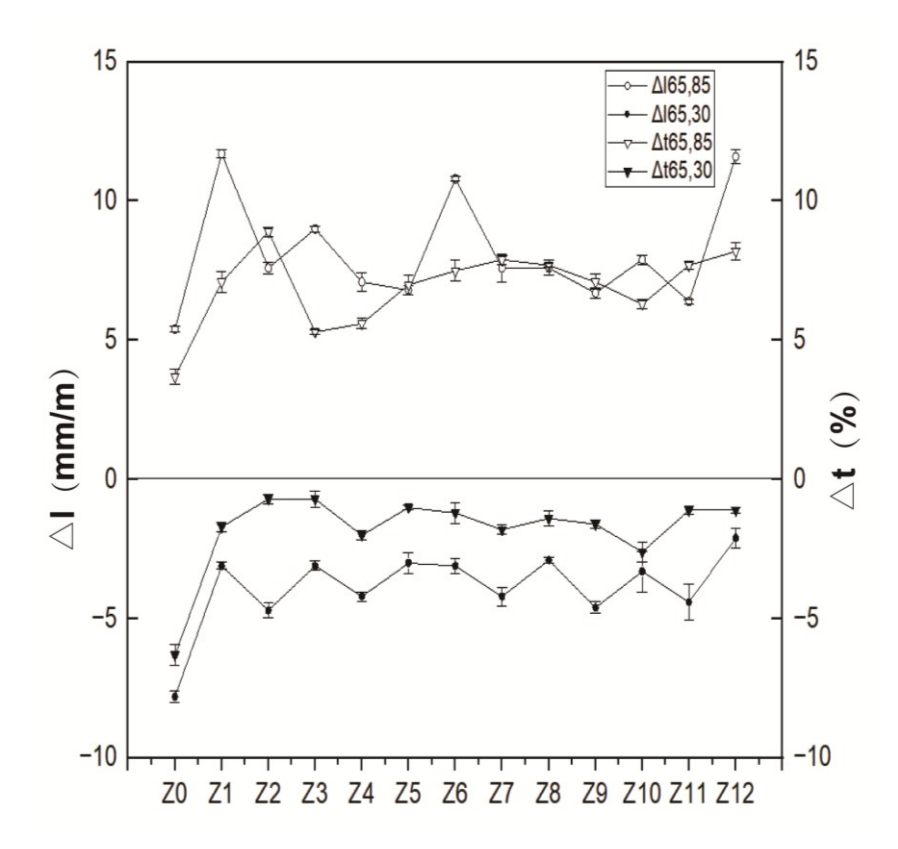


Fig. 4. Effect of different flame retardants on water absorbency of TP/BF composites

Mechanical Properties

Figure 5 shows the effects of different flame-retardant systems on the mechanical properties of TP/BF composites. Compared to the untreated specimens, the elastic modulus of flame-retardant-treated TP/BF composites decreased by 42.4% to 81.2%, the static bending strength decreased by 8.5% to 64.8%, and the internal bond strength decreased by 5.8% to 57%. It is evident that the mechanical properties of the treated specimens declined to varying degrees after flame-retardant treatment, with the extent of reduction primarily depending on factors such as the type of flame retardant and its compatibility with the composite matrix.

For the Z1 group treated with boric acid/borax, the mechanical strength decreased significantly. This may be attributed to the disruption of the synergistic effect of the "fiber-adhesive-overall structure" by the addition of boric acid/borax. This was manifested as interference with adhesive curing, weakening of fiber strength, reduced interfacial bonding efficiency between fibers and adhesive, and increased porosity of the composite. These factors ultimately made the specimens more prone to fracture or deformation under stress (Wang *et al.* 1996; Ünal *et al.* 2023). Kumar *et al.* (2022) also confirmed this phenomenon, noting that the addition of boric acid/borax to wood-plastic composites significantly reduced their strength, with the extent of mechanical performance decline influenced by the content of boric acid/borax.

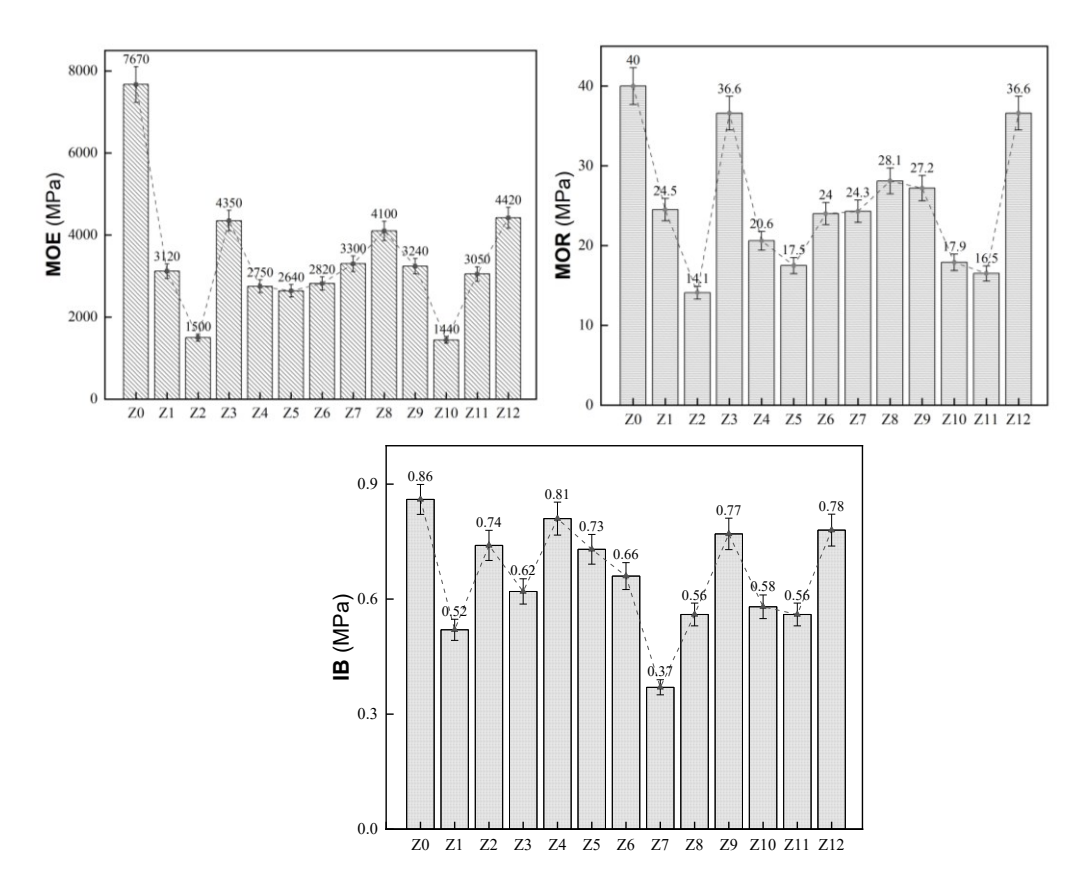


Fig. 5. Effect of different flame retardants on MOE, MOR and IB of TP/BF composites

The Z2 group, treated with nano-SiO, also exhibited a substantial decline in mechanical strength. Although some studies (Ma et al. 2020; Xu 2022; Zhao et al. 2024) suggest that nano-SiO₂ can enhance the mechanical properties of composites to some extent, in this study, the small amount of nano-SiO₂ added may have failed to improve the mechanical properties of TP/BF composites effectively. Additionally, the dispersant used—trisodium phosphate solution—exhibited strong alkalinity due to the intense hydrolysis of phosphate ions, almost completely decomposing into disodium hydrogen phosphate and sodium hydroxide in water. This could damage the wood fiber structure, and sodium hydroxide could react with the phenolic hydroxyl and aldehyde groups in the phenolic resin adhesive, leading to the breakage of molecular chains and weakening the bonding effect, thereby reducing mechanical strength (Hu 2023; Bai et al. 2024). In the Z3 group, both magnesium hydroxide and aluminum hydroxide are irregular flake crystals with strong polarity, resulting in poor interfacial compatibility with the plastic matrix and a tendency to agglomerate. This hindered particle dispersion within the matrix, leading to stress concentration under load and a consequent decline in the composite's mechanical strength (Liu 2018; Ma 2020). The flame retardant in the Z4 group mainly consisted of ammonium polyphosphate (APP). As an inorganic polymer, APP contains a large number of phosphate ions in its molecular structure. Its addition to the composite lowered the adhesive's pH, catalyzing polycondensation and promoting the formation of cross-linked structures. However, the poor compatibility between APP and the composite adversely affected the bonding strength between phenolic resin and fibers, leading to reduced mechanical strength (Lu and Lu 2023; Mao 2023). The Z5 group also exhibited a

decline in mechanical performance due to the poor compatibility between disodium octaborate tetrahydrate and the matrix material, as well as its tendency to reduce the composite's ability to undergo plastic deformation. Among other specimens modified with different flame-retardant systems, it was observed that the MOE, MOR, and IB of TP/BF composites varied significantly depending on the flame-retardant formulation used. Overall, among single flame-retardant systems, magnesium hydroxide and aluminum hydroxide (Z3) had a relatively smaller impact on the composite's MOE, MOR, and IB. Among composite flame-retardant systems, Z12 had the least impact, followed by Z8 and Z9.

Among them, the TP/BF composites modified by flame retardants Z3 (magnesium hydroxide/aluminum hydroxide), Z8 (boric acid/borax/ammonium polyphosphate/ disodium octaborate tetrahydrate), Z9 (boric acid/borax/trisodium phosphate/nano-silica), and Z12 (boric acid/borax/ammonium polyphosphate/disodium octaborate tetrahydrate/ trisodium phosphate/nano-silica/magnesium hydroxide/aluminum hydroxide) could meet the usage requirements of ordinary, furniture and building medium-density fiberboards under different conditions specified in GB/T 11718 - 2021.

FTIR Analysis of Flame Retardant Composites

The FTIR spectra of flame-retardant-treated and untreated samples meeting the B1-grade requirements are shown in Fig. 6. Some characteristic absorbance peaks were observed in all treated specimens. The stretching vibration peak at 3420 cm⁻¹ was attributed to hydroxyl groups (-OH), and the stretching vibration peak at 2920 cm⁻¹ was attributed to methylene (-CH₂-), which were the characteristic peaks of cellulose (Lou et al. 2021). The symmetric stretching vibration peak at 2850 cm⁻¹ was attributed to methylene (-CH₂-) from polyethylene in Tetra Pak (Sun 2015). From 1730 to 1800 cm⁻¹, stretching vibration peaks indicated C=O bonds in esters, acids, ketones, and amides, which would have been primarily from lignin in bamboo fibers and paper fibers in Tetra Pak (Guo et al. 2019). The absorbance peaks at 1610 cm⁻¹ and 870 cm⁻¹ were caused by C=C stretching vibrations and =CH out-of-plane bending vibrations in the benzene ring of phenolic resin (Bai et al. 2024). Two characteristic peaks caused by bending vibrations of CH₃ and CH₂ at 1460 cm⁻¹ and 1430 cm⁻¹ were attributed to the saturated alkane chains within the fibers. The multiple absorption peaks at 1300 to 1025 cm⁻¹ corresponded to the esters, alcohols, and ethers, arising from C-O stretching vibrations (Wang et al. 2020). Compared to the untreated samples (Z0), the Z3 and Z12 groups exhibited a new stretching vibration peak at 3700 cm⁻¹, attributed to the -OH stretching vibration in magnesium hydroxide and aluminum hydroxide. The Z9 and Z12 groups showed a characteristic peak at 1100 cm⁻¹, caused by the asymmetric stretching vibration of Si-O-Si. Peaks at 1100 to 1050 cm⁻¹ were due to the asymmetric stretching vibration of PO₄³⁻ in trisodium phosphate. In the Z8 and Z12 groups, peaks in the 1100 to 1050 cm⁻¹ range were attributed to the asymmetric stretching vibration of PO₄³⁻ in ammonium polyphosphate (APP). The absorbance peak at 1200 cm⁻¹ was caused by the B-O stretching vibration in borates (Wang et al. 2020). In summary, bamboo fibers, Tetra Pak components, and various flame retardants were chemically bonded with different functional groups under the action of phenolic resin, which was the fundamental reason for the improved flame retardancy of the TP/BF composites.

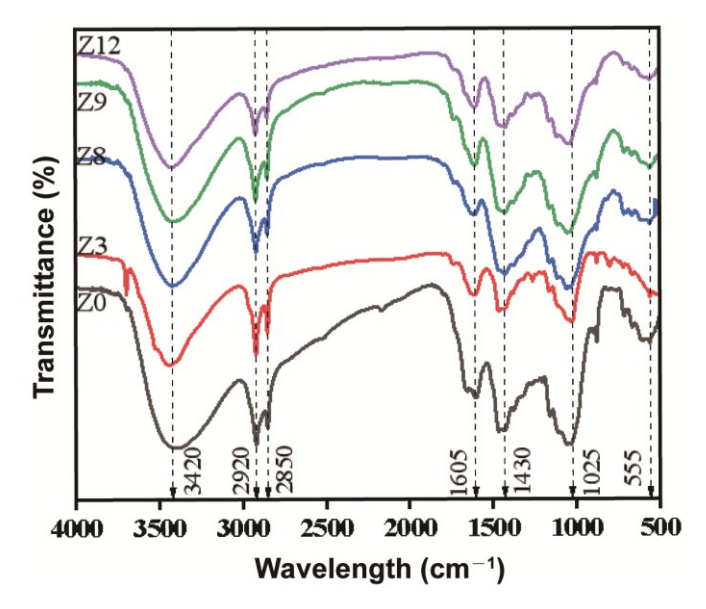


Fig. 6. FTIR spectra of TP/BF composites with promising flame retardant modification

In the future, with the optimization of processes (such as interface modification and high-efficiency flame retardant synergy), TP/BF would be expected to become widely used in fields such as building formwork, furniture panels and packaging buffer materials, becoming a typical example of circular economy and green manufacturing.

CONCLUSIONS

- 1. Waste Tetra Pak (TP) and bamboo fiber (BF) were used as the main raw materials to prepare TP/BF composites by constructing different inorganic flame-retardant systems. This approach adheres to the concept of "treating waste with waste and supplementing green with green" to achieve the multiple goals of "waste reduction resource recycling material functionalization industrial greening". The significance of this research not only lies in solving problems such as Tetra Pak pollution and bamboo waste, but also in exploring a technical path for upgrading low-value waste to high value and functionalizing natural resources, providing an innovative solution that integrates environmental protection, economy and practicality for the development of global sustainable packaging.
- 2. Different inorganic flame retardant components had significant differences in their impact on the flame-retardant effect of the composites. Compared with the untreated control samples, the flame-retardant ability of the samples with a single flame-retardant system varied to different degrees, with the highest limiting oxygen index reaching 36.2%. The samples with the compound flame-retardant system all showed improvements to varying degrees, with the maximum limiting oxygen index reaching 37.6%. Combined with the above judgment standards and industry consensus, the limiting oxygen index of both the samples with the single flame-retardant system and the samples with the compound flame-retardant system in this study was significantly higher than the general threshold of 32% for Grade B1 wood-based panels, and meets the clear requirement that "an OI ≥ 32.5% indicates compliance with Grade B1-C

- specified in GB 8624-2012". This demonstrates that all composite materials treated with inorganic flame retardants reached the general Grade B1 flame-retardant level in the wood-based panel industry.
- 3. The addition of flame retardants had a negative impact on the mechanical properties and dimensional stability of the composites, and the degree of impact varied depending on the type, nature, and content of the flame retardants. Compared with the untreated samples, the flexural strength of the flame-retardant treated samples decreased by 8.5 to 64.8%, the elastic modulus decreased by 42.4 to 81.2%, the internal bonding strength decreased by 5.8 to 57%, the water absorption decreased by 17.4 to 36.1%, and the 24-h water absorption thickness expansion increased by 11.3 to 137.8%. Among them, the TP/BF composites modified by the inorganic flame retardant systems of Z3, Z8, Z9, and Z12 could meet the usage requirements of ordinary, furniture, and building medium-density fiberboards under different conditions specified in GB/T 11718 (2021).
- 4. Fourier transform infrared (FTIR) analysis showed that the methylene groups on the polyethylene in Tetra Pak undergo stretching vibration, the hydroxyl groups in the fibers undergo stretching vibration and asymmetric stretching vibration, and the C=C bonds on the benzene ring of the phenolic resin undergo stretching vibration. Such information helps to confirm other findings of this work.

ACKNOWLEDGEMENTS

The authors are grateful for the financial support of Forestry Science and Technology Innovation Projects of Hubei Province (2025LKZC04), Central Financial Promotion Project (2024TG24), and National Training Program of Innovation and Entrepreneurship for Undergraduates (202410057028).

REFERENCES CITED

- Abdul Khalil, H. P. S., Davoudpour, Y., Saurabh, C. K., Hossain, M. S., Adnan, A. S., Dungani, R., Paridah, M. T., Mohamed, Z. I. S., Fazita, M. R. N., and Syakir, M. I. (2016). "A review on nanocellulosic fibres as new material for sustainable packaging: Process and applications," *Renewable and Sustainable Energy Reviews* 64, 823-836. DOI: 10.1016/j.rser.2016.06.072.
- Amorim, C. F., Carvalho, L. F., and Junior, C. R. (2024). "Investigation of the mechanical properties of polymer based on Tetra Pak waste," *Journal of the Brazilian Society of Mechanical Sciences and Engineering* 46(12), 679.
- Aranda-García, F. J., González-Pérez, M. M., Robledo-Ortíz, J. R., Sedano-de la Rosa, C., Espinoza-Herrera, K., and Ramírez-Arreola, D. E. (2020). "Influence of processing time on physical and mechanical properties of composite boards made of recycled multilayer containers and HDPE," *Journal of Material Cycles and Waste Management* 22(6), 1-9. DOI: 10.1007/s10163-020-01092-5

- Bai, Y., Bai, F., Zhang, L., and co-authors. (2024). "Preparation and process optimization of lignin-based phenol-formaldehyde resin," *Chemical Industry and Engineering Progress* 43(2), 1033-1038.
- Bal, B. C. (2022). "Mechanical properties of wood-plastic composites produced with recycled polyethylene, used Tetra Pak® boxes, and wood flour," *BioResources* 17(4), 6569-6577. DOI: 10.15376/biores.17.4.6569-6577
- Bekhta, P., Lyutyy, P., and Hiziroglu, S. (2016). "Properties of composite panels made from Tetra-Pak and polyethylene waste material," *Journal of Polymers and the Environment* 24(2), 159-165.
- Chen, H. Y. (2011). AFM Characterization of Interfacial Hygroscopicity and Interfacial Properties of Bamboo Strip/Vinyl Ester Composites, Master's Thesis, Donghua University, Shanghai, China.
- Ding, Z., Xu, X., Phan, T., Hu, X., and Nie, G. (2018). "High adsorption performance for As(III) and As(V) onto novel aluminum-enriched biochar derived from abandoned Tetra Paks," *Chemosphere* 208, 800-807. DOI: 10.1016/j.chemosphere.2018.06.050
- Dou, Y., Yu, X., and Iwamatsu, F. (2011). "Current situation and development countermeasures of bamboo resources exploitation and utilization in China," *Chinese Journal of Agricultural Resources and Regional Planning* 32(5), 65-70.
- Dreizin, E. L. (1999). "Internal heterogeneous processes in aluminum combustion," in: *Fifth International Microgravity Combustion Workshop*.
- Ebadi, M., Farsi, M., Narchin, P., and Madhoushi, M. (2016). "The effect of beverage storage packets (Tetra PakTM) waste on mechanical properties of wood-plastic composites," *Journal of Thermoplastic Composite Materials* 29(12), 1601-1610. DOI: 10.1177/0892705715618745
- Fang, L., Lu, X., Zeng, J., Chen, Y., and Tang, Q. (2020). "Investigation of the flame-retardant and mechanical properties of bamboo fiber-reinforced polypropylene composites with melamine pyrophosphate and aluminum hypophosphite addition," *Materials (Basel)* 13(2), article 479. DOI: 10.3390/ma13020479
- GB 8624-2012. (2012). "Classification of Combustion Performance of Building Materials and Products." Beijing: China Standards Press.
- GB 8624-2012 (2012). "Classification for burning behavior of building materials and products," China Standards Press Beijing, China.
- GB/T 11718-2021 (2021). "Medium density fibreboard," China Standards Press Beijing, China.
- GB/T 2406.2-2009 (2009). "Plastics Determination of burning behaviour by oxygen index Part 2: Ambient-temperature test," China Standards Press Beijing, China.
- Guo, W., Kalalia, E. N., Wang, X., Xing, W., Zhang, P., Song, L., and Hu, Y. (2019). "Processing bulk natural bamboo into a strong and flame-retardant composite material," *Industrial Crops and Products* 138, 111478. DOI: 10.1016/j.indcrop.2019.111478
- Hu, H. D. (2023). "Research progress on flame-retardant wood-plastic composites based on polyolefin," *Shanxi Chemical Industry* 43(1), 40-41, 44.
- Jiang, R., Xu, Y. F., Yang, X. J., Zhang, L., Fan, Z. Y., Guo, X. Y., Guo, H., Sun, B. Q., and Yu, L. L. (2025). "Effects of hot-pressing parameters on the properties of waste Tetra Pak/bamboo composites," *BioResources* 20(1), 826-841. DOI: 10.15376/biores.20.1.826-841

- Kolyada, L. G., Smirnova, A. V., and Tarasyuk, E. V. (2021). "Development of new composite materials from Tetra Pak packaging waste," *Solid State Phenomena* 316, 3-8. DOI: 10.4028/www.scientific.net/SSP.316.3.
- Kongkraireug, N., Chuayjuljit, S., Chaiwutthinan, P., Larpkasemsuk, A., and Boonmahitthisud, A. (2018). "Use of magnesium hydroxide as flame retardant in poly(lactic acid)/high impact polystyrene/wood flour composites," *Key Engineering Materials* 773, 311-315. DOI: 10.4028/www.scientific.net/KEM.773.311
- Kumar, R., Gunjal, J., and Chauhan, S. (2022). "Effect of borax-boric acid and ammonium polyphosphate on flame retardancy of natural fiber polyethylene composites," *Maderas. Ciencia y Tecnología* 24(34). DOI: 10.4067/s0718-221x2022000100434
- Lan, P., Yang, R., Li, W., & Ji, Y. (2018). "Effect of inorganic magnesium aluminum hydroxide flame retardant on flame retardant properties of medium density fiberboard," *Journal of Northwest Forestry University* 33(2), 203-208.
- Li, H., Chen, M., Hu, L., Wang, X., Gu, Z., Li, J., and Yang, Z. (2023a). "Optimization design of bamboo filament decorated board process based on response surface," *BioResources* 18(1), 73-86. DOI: 10.15376.18.1.73.76
- Li, J., Zhu, Y., Bian, R., Wei, Y., Jiang, S., Li, K., Li, X., Tian, D., Zhan, X., Li, J. (2023b). "Construction of a boron nitride nanosheet hybrid for tough, strong, and flame-retardant phenolic resins," *Chemical Engineering Journal* 471, article 144463. DOI: 10.1016/j.cej.2023.144463
- Li, L., Wei, B., Cao, Y., and Yang, S. (2024a). "Preparation of high performance thermal conductive composites from aluminum plastic packaging waste *via* solid-state drawing," *Polymer* 306, article 127185. DOI: 10.1016/j.polymer.2024.127185
- Li, Y., Yang, X., Lu, Z., *et al.* (2024b). "Research progress on the application of ammonium polyphosphate in flame retardancy," *Inorganic Chemicals Industry* 56(5). DOI: 10.19964/j.issn.1006-4990.2023-0442
- Li, Z., and Lv, L. (2022). "Flame retardant properties of ammonium polyphosphate treated straw/polycaprolactone composites," *Shanghai Textile Science & Technology* 50(10), 22-24 + 30.
- Liu, H. R., Yang, X. M., Zhang, X. B., Su, Q., and Zhang, F. D. (2021). "Tensile shear bonding properties of bamboo flattened panels," *Journal of Forestry Engineering* 6(1), 68-72.
- Liu, N. (2018). Study on Combustion Behavior and Mechanical Properties of Polyolefin Composites Flame-retarded by Intumescent Flame Retardants Synergized with Magnesium Hydroxide/Aluminum Hydroxide, Master's Thesis, Southwest Jiaotong University, Chengdu, China.
- Liu, W. G., Cao, Q. Y., Ni, E. L., Cao, C. L., Lin, L. B., Chen, Y. M., Zhang, J., and Li, Y. (2024). "Preparation of modified carbon material from waste Tetra Pak and its application in treatment of chromium containing wastewater," *Environmental Science & Technology* 2024(S2), 160 167.
- Lokahita, B., Takahashi, F., Yoshikawa, K., and Aziz, M. (2017). "Energy and resource recovery from Tetra Pak waste using hydrothermal treatment," *Applied Energy* 207, 107-113. DOI: 10.1016/j.apenergy.2017.05.141
- Lou, C., Zhou, Y., Yan, A., and Liu, Y. (2021). "Extraction of cellulose from corn-stalk taking advantage of pretreatment technology with immobilized enzyme," *RSC Advances* 12(2), 1208-1215. DOI: 10.1039/D0RA08975K

- Lu, Y. X., and Lu, L. G. (2023). "Flame retardant and mechanical properties of ammonium polyphosphate-tannic acid-melamine/epoxy resin composites," *Materials Reports* 37(9), article 21090236-8. DOI: 10.11896/cldb.21090236
- Ma, P. (2020). Preparation and Performance Study of Polypropylene-based Construction Formwork, Ph.D. Dissertation, Shenyang Jianzhu University, Shenyang, China.
- Ma, Y., He, H., Huang, B., Jing, H., and Zhao, Z. (2020). "*In situ* fabrication of wood flour/nano silica hybrid and its application in polypropylene-based wood-plastic composites," *Polymer Composites* 41(2), 573-584. DOI: 10.1002/pc.25389
- Mao, W. (2023). Study on Layered Flame Retardant Preparation Technology and Properties of Large-Flake Particleboard, Ph.D. Dissertation, Nanjing Forestry University, Nanjing, China.
- Martínez Barrera, G., and Escobar Campos, C. U. (2024). "Waste Tetra Pak beverage containers as reinforcement in polymer concrete," *EducateConCiencia* 32(3), 1-20.
- Meng, X. F. (2020). Study on Flame Retardant Properties of Expandable Flameretardant Polystyrene Synergized with Silica, Master's Thesis, Harbin University of Science and Technology, Harbin, China.
- Muñoz-Vélez, M. F., Hidalgo-Salazar, M. A., and Mina-Hernández, J. H. (2018). "Content and surface modification of fique fibers on the properties of a low-density polyethylene (LDPE)-Al/fique composite," *Polymers* 10(10), article 1050. DOI: 10.3390/polym10101050
- Nie, S., Fang, C., Xu, Y., et al. (2022). "Water resistance, flame retardancy, and thermal properties of hydrophobic polypropylene/bamboo fiber composites," *Journal of Thermal Analysis and Calorimetry* 147(22), 12547-12559.
- Riedewald, F., Wilson, E., Patel, Y., Vogt, D., Povey, I., Barton, K., Lewis, L., Caris, T., Santos, S., O'Mahoney, M., and Sousa-Gallagher, M. (2022). "Recycling of aluminium laminated pouches and Tetra Pak cartons by molten metal pyrolysis—Pilot-scale experiments and economic analysis," *Waste Management* 138, 172-179. DOI: 10.1016/j.wasman.2021.11.049
- Santhanam, P. R., Hoffmann, V. K., Trunov, M. A., and Dreizin, E. L. (2010). "Characteristics of aluminum combustion obtained from constant-volume explosion experiments," *Combustion Science and Technology* 182(7) 904-921. DOI: 10.1080/00102200903418278
- Shi, Y. (2017). Study on Flame Retardant Properties of Pine Wood Treated with Ammonium Polyphosphate Modified and Compound Flame Retardants, Master's Thesis, Southwest Petroleum University, Chengdu, China.
- Sun, X. (2015). Study on Preparation and Interfacial Bonding Properties of Waste Tetra Pak/wood Chip Particleboard, Master's Thesis, Beijing Forestry University, Beijing, China.
- Ünal, H., Yetgin, S. H., and Köse, S. (2023). "Determination of mechanical performance of boric acid filled polypropylene-based polymer composites," *Journal of Scientific Reports-A* 55, 185-192. DOI: 10.59313/jsr-a.1354200
- Wang, G., Chen, F. M., Cheng, H. T., and Fu, J. H. (2020). "Special advantage and innovative development of bamboo industry in China," *World Bamboo and Rattan* 18(6), 6-13, 29. DOI: 10.12168/sjzttx.2020.06.002
- Wang, J. H., Yuan, F., Liu, Z. J., Qin, X. F., and Zhou, H. X. (2020). "Effect of APP-PER-MEL flame retardant on properties of bamboo powder/PP composites," *Journal of Northwest Forestry University* 35(4), 212-217.

- Wang, Y., Simonsen, J., Neto, C. P., Rocha, J., Rials, T. G., and Hart, E. (1996). "The reaction of boric acid with wood in a polystyrene matrix," *Journal of Applied Polymer Science* 62, 501-608.
- Way, D., Kamke, F. A., and Sinha, A. (2020). "Moisture transport in wood-based structural panels under transient hygroscopic conditions," *Forest Products Journal* 70(3), 283-292. DOI: 10.13073/FPJ-D-19-00042
- Xu, W. H. (2022). "Study on properties of nano-silica/organophosphorus synergistic flame-retardant wood-plastic composites," *China Forest Products Industry* 59(2), 13-16, 27.
- Ye, C., Qian, Q., and Cao, C. (2022). "High-value recycling and utilization of Tetra Pak under the goal of carbon neutrality," *Renewable Resources and Circular Economy* 15(2), 34-38.
- Zhao, Y. (2024). "Preparation and flame retardancy of wood flour/polypropylene composites synergistically modified by compound flame retardants," *Plastics Science and Technology* 52(1), 67-70.
- Zhao, Z., Li, X., Rui, C., and Liu, M. (2024). "Research progress on application of environment-friendly compound flame retardants in wood-plastic composites," *Engineering Plastics Application* 52(3), 186-191.
- Zhou, Z. X. (2018). Study on Main Properties of Bamboo Treated with Water-Based Flame Retardant, Ph.D. Dissertation, Zhejiang A & F University, Hangzhou, China.
- Zúñiga-Muro, N. M., Bonilla-Petriciolet, A., Mendoza-Castillo, D. I., Duran-Valle, C. J., Silvestre-Albero, J., Reynel-Ávila, H. E., and Tapia-Picazo, J. C. (2021). "Recycling of Tetra Pak wastes *via* pyrolysis: Characterization of solid products and application of the resulting char in the adsorption of mercury from water," *Journal of Cleaner Production* 291, article 125219. DOI: 10.1016/j.jclepro.2020.125219

Article submitted: August 17, 2025; October 5, 2025; Revised version received and accepted: October 6, 2025; Published: October 10, 2025.

DOI: 10.15376/biores.20.4.10228-10248